Fluid flow through Apollonian packings

Rafael S. Oliveira,[1] José S. Andrade, Jr.,[2] and Roberto F. S. Andrade[1]
[1]*Instituto de Física, Universidade Federal da Bahia, 40210-210 Salvador, Brazil*
[2]*Departamento de Física, Universidade Federal do Ceará, Campus do Pici, 60455-760 Fortaleza, Brazil*
(Received 22 December 2009; revised manuscript received 25 February 2010; published 7 April 2010)

This work considers the flow of a Newtonian fluid in a two-dimensional channel filled with an array of obstacles of distinct sizes that models an inhomogeneous medium. Obstacle sizes and positions are defined by the geometry of an Apollonian packing (AP). The radii of the circles are uniformly reduced by a factor $s<1$ for assemblies corresponding to the five first AP generations. The region of validity of Darcy's law as a function of the channel Reynolds number is investigated for different values of s and the dependency of the flow pattern and permeability with respect to porosity is established. Our results show that the semiempirical Kozeny-Carman scaling relation is satisfied provided the effects of the apparent porosity and s-dependent formation factor are properly considered.

DOI: 10.1103/PhysRevE.81.047302 PACS number(s): 47.56.+r, 05.45.Df, 47.11.−j, 47.53.+n

The flow through a porous medium [1–3] is of importance in many practical situations ranging from oil recovery [4,5] to chemical reactors [6] and has been the object of study for a long time in various fields of science and engineering. In many practical situations, the analysis of flow in porous media requires a knowledge of how the flow varies with the pressure gauge. The determination of this relationship is only possible if some physical quantity that represents the resistance of flow through porous media is known. This resistance can be expressed in various ways, e.g., for single-phase fluid flow, the friction factor or the Darcy permeability k [1–3], which is related to the average flow velocity v, viscosity μ, and pressure drop ΔP over a channel segment of length L by

$$v = -\frac{k}{\mu}\frac{\Delta P}{L}. \tag{1}$$

With the huge advance of numerical methods in computational fluid dynamics (CFD) [7,8], numerical simulations based on detailed models of pore geometry and fluid flow have been used to predict permeability coefficients as well as to validate semiempirical correlations obtained from real porous materials. One useful approach consists to investigate how the presence of obstacles placed in a channel influences the value of k. Until now, most studies have considered the presence of equally shaped obstacles randomly distributed in a regular channel [9–13]. Although results for three-dimensional models have more direct relationship to actual cases, studies considering simpler two-dimensional situations are able to provide results that are insightful and easier to visualize.

In this work, we investigate the behavior of a fluid flowing through a channel with obstacles of different sizes, distributed in a nonperiodic array. Such requirements can be geometrically defined by means of an Apollonian packing (AP) [14]. In two dimensions, such geometrical construction entirely blocks the flow if maximum tangent circles are considered. Thus, the radii of the circles must be multiplied by a factor $0 \le s < 1$ in order to allow for the fluid to flow. The flow properties depend on the porosity (or void fraction) $\phi = \phi(s,g)$, where g denotes the *finite* AP construction generation. It is important to notice that, once a given value of ϕ can be obtained by adequately tuning distinct values of s and g, the bare value of ϕ is not sufficient to characterize such flow properties. Indeed, our calculations show that these are influenced by the generation g and the reduction factor s in quite different ways. Our main finding is to show that a scaling relation between k and ϕ is valid provided we use a generalized form of the Kozeny-Karman (KC) relation [2,15–18]. Of course such relation is limited to the range of validity of Darcy's law, which can be expressed in terms of the largest value $\mathrm{Re}_{\max}$ for which Eq. (1) is verified. Here, Re denotes the channel Reynolds number, as we define later.

Under the assumption of the validity of Darcy's law, the equivalent resistance and the permeability of a porous medium has been previously modeled as an AP in the lubrication approximation [19,20]. Due to the scaling invariance, it was possible to derive a recurrence relation between these quantities for successive values of g. However, this type of approach does not fully account for fluid dynamical details of the flow at the pore level.

The geometrical setup for our CFD investigation consists of a two-dimensional channel of height H and length $L=32H$, with a constant pressure gauge ΔP_0 forcing the fluid to displace from left to right. A fixed coordinate system is placed at the center of the channel, so that the coordinates of the channel corners are $(\pm L/2, \pm H/2)$. The obstacles are placed only in the square limited by the points $(\pm H/2, \pm H/2)$. Initially four equally sized tangent circles of radius $R_{g=1}=H/4$ are placed inside the channel, so that their centers lie on the points $C_1(\pm H/4, \pm H/4)$. In the second generation $g=2$, three new circles are added: the first one, with radius $R_2=H/9.697$, has its center at the origin of our coordinate system. The centers of the other circles of radius $R_2=H/16$ are placed at the points $C_2=(0, \pm H/2.286)$. For $g>2$, one tangent circle is added to each free space bounded by three tangent circles. In this process, we consider the channel walls as circles of infinite radius with centers placed at the infinite.

The solution to this problem is provided by the *Descartes Circle Theorem* and *Complex Descartes Theorem* [21,22]: given three mutually tangent circles in three distinct points, the curvature of which expressed in terms of their radii R_1,

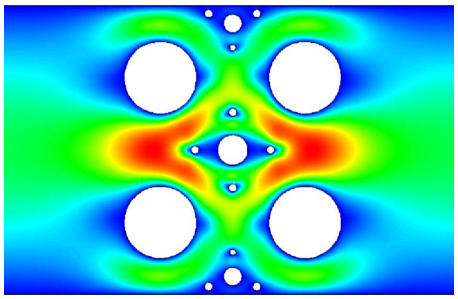

FIG. 1. (Color online) Model of a porous media with obstacles of different sizes based on an AP, together with typical flow pattern through the packing for $s=0.5$ and $g=3$. The colors ranging from blue (dark) to red (light) correspond to low and high velocity magnitudes, respectively. Preferential channels depend more strongly on g than on s.

R_2, and R_3 by $b_j=1/R_j$, there exists two circles that are tangent to each one of the them. Their curvatures b_4 are given by the roots of

$$\sum_{j=1}^{4} b_j^2 = \frac{1}{2}\left(\sum_{j=1}^{4} b_j\right)^2. \tag{2}$$

Further, the coordinates (x_j, y_j) of the centers of each of such four tangent circles satisfy

$$\sum_{j=1}^{4} (b_j z_j)^2 = \frac{1}{2}\left(\sum_{j=1}^{4} b_j z_j\right)^2, \tag{3}$$

where $z_j=x_j+iy_j$. The b_4 solutions of Eq. (2) fulfill the following oriented circle convention: the normal at the circle tangent point has a positive curvature if it is directed outwards, and a negative curvature if it is directed inwards. Thus, a negative b_4 corresponds to the external circle containing three circles in its interior. The geometry of our model is shown in Fig. 1, for $s=0.5$ and $g=3$. Note that the position of the circle centers are left unchanged when the radii are multiplied by $s<1$.

As anticipated, the porosity ϕ depends both on the reduction parameter s and on the packing generation g. This is illustrated in Fig. 2, where we draw the dependence of ϕ with respect to s for different values of g. As we will see, despite the fact that the differences in ϕ become smaller for larger values of g, these small obstacles produce relevant changes in the flow patterns. We considered $s \in [0.3, 0.9]$, and $g=1$, 2, 3, 4, and 5. When $g=5$, the packing encompasses 137 circles, and the ratio of the smallest to the largest circle radius is 1/97.

The detailed fluid dynamics through the pore space delimited by the AP is calculated considering steady-state flow and incompressibility in a two-dimensional framework. This is obtained by numerical integration of the continuity and Navier-Stokes equations,

$$\nabla \cdot \vec{v} = 0, \tag{4}$$

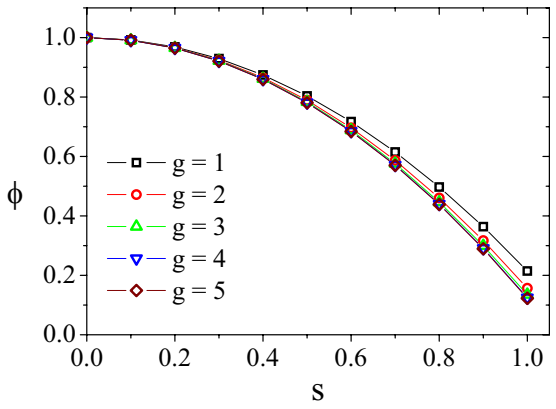

FIG. 2. (Color online) Dependence of porosity ϕ with respect to the reduction factor s for several values of g. The differences in the values of ϕ for fixed values of s decreases as g increases, as the radii of latter generations circles become smaller.

$$\rho\vec{v} \cdot \nabla\vec{v} = -\nabla P + \mu\nabla^2\vec{v}, \tag{5}$$

where ρ is the fluid density. Here, we consider overall nonslip boundary conditions at the channel walls and at all obstacle surfaces. The boundary conditions are constant velocity at the channel inlet v_i and constant pressure at the outlet. This geometry defines the channel Reynolds number $\mathrm{Re}=\rho v_i H/\mu$. To obtain a more accurate measure of the AP influence on the flow, and to avoid the possible presence of back flow effects, the calculation of the overall pressure drop is based on the average pressure values at $x=-3H/2$ and $x=5H/2$.

The solution of Eqs. (4) and (5) for the velocity and pressure fields in the whole domain is obtained through discretization by means of the control volume finite-difference technique within a CFD environment [23]. Due to a strong reduction in the circle radii as g increases, the integration of Eqs. (4) and (5) within the channel central square must be carefully done. When s is large, most difficulties are related to establishing a mesh within the narrow channels. On the other hand, when s is small, it becomes difficult to keep the precise geometrical features of very small circles, specially for larger values of g. In both situations, the demand for very fine meshes constitutes the computational limiting step of the integration process. Here, we use unstructured meshes, locally adapted to the constraints expressed by the proper boundary conditions and convergence of the numerical solutions [24].

Some typical flow patterns resulting from the numerical integration are shown in Fig. 1. The flow through the central part of the packing is clearly favored. However, the presence of small circles introduced at larger steps of construction of the packing are effective in deviating the flow through the larger channels lying at larger distances from the channel center.

To broaden the range of our discussion, it is convenient to consider also the dependence between ΔP and v beyond the $\mathrm{Re}_{\max}$ limit. In such case, nonlinear corrections to Darcy's law are needed to correlate flow properties. The approach we adopt here is to use the ansatz

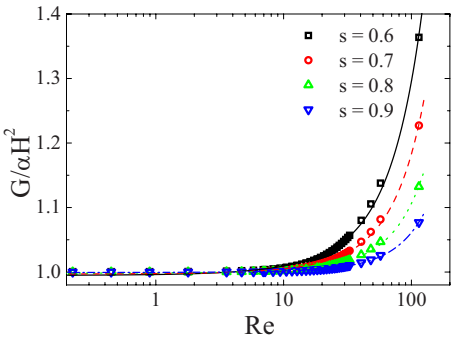

FIG. 3. (Color online) The hydraulic resistance G as a function of Re for different values of s and $g=5$. Symbols indicate the values at the left-hand side of Eq. (6), while lines indicate the values obtained by quadratic expansion. To plot all curves in the same axis, G has been divided by α. Better accordance is achieved when s increases and channels become narrower.

$$G = \alpha H^2 + \beta H \mathrm{Re} + \gamma \mathrm{Re}^2, \tag{6}$$

where $G=-\Delta P H^2/\mu v L$ is a dimensionless measure of the hydraulic resistance [25]. The coefficient α corresponds to the reciprocal of the linear permeability of the porous material, and the two remaining terms with coefficients β and γ can be interpreted, respectively, as second and third order corrections that should account for the contribution of inertial forces in the fluid flow. For sufficiently low Re, Eq. (6) reduces to Darcy's law.

The values of the coefficients α, β and γ have been obtained by the least-squares method, while the results for G/α are illustrated, for $g=5$, in Fig. 3. As the values of the coefficient of the cubic term are always much smaller than those of the quadratic term, we conclude that a generalized permeability that incorporates second order corrections is sufficient to describe the flow in the range of Re numbers of interest.

Several expressions have been proposed to quantitatively express k in Darcy's Eq. (1), as a function of the medium physical features. Among them, the most simple one is the KC expression $k=c_0\phi^3/S_v^2$, where ϕ is the only independent variable. Here, c_0 is the so-called KC constant, observed to lay in an interval $\sim[0.2,0.7]$, while S_v, the specific surface per unit volume, can be expressed in terms of the specific surface per unit solid material S_0 as $S_v=S_0(1-\phi)$. With the knowledge of the range of validity of Eq. (1), the values of k are evaluated for the selected values of s and g. In Fig. 4(a), we show the dependence of k/k_0 with respect to ϕ for different values of g, where $k_0=H^2/12$ represents the empty channel permeability. As expected, k assumes distinct values when we hold ϕ fixed but compare different values of g. The absolute difference becomes relevant in the region of large ϕ (small s), when the smaller circles introduced in the latter generations cause significant changes in the flow patterns.

To verify whether the nonlinear dependence between k and ϕ can be explained by the quoted semiempirical KC expression, we have to investigate the dependence of k/k_0 with respect to $\phi^3/(1-\phi)^2$. Here we must take into account the fact that $\phi=\phi(s,g)$, and explore the scaling relation when one parameter changes and the other remains constant.

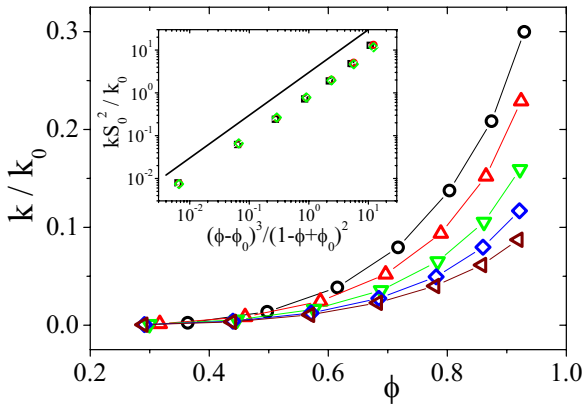

FIG. 4. (Color online) The main panel shows the dependence of k/k_0 with respect to ϕ for successive packing generations $g=1$ (circles), 2 (triangles up), 3 (triangles down), 4 (diamonds), and 5 (triangles left). In the inset, dependence of kS_0^2/k_0 with respect to $(\phi-\phi_0)^3/(1-\phi+\phi_0)^2$ for $g=3,4$, and 5, where $\phi_0=\phi(s=1,g)$. The straight line with slope 1.0 clearly shows that Eq. (7) holds with very high degree of accuracy. Symbols for $g=3,4$, and 5 are, respectively, square, circle, and diamond. In both plots, $\phi=\phi(s,g=\text{const})$.

However, it is important to recall that two corrections must be taken into account to adequately deal with the presence of obstacles of different sizes. In first place, Fig. 2 shows that, for finite values of g, the porosity does not vanish when $s\equiv 1$, what contrasts with the requirement that k must vanish in this same limit. Thus, to meet this condition, we introduce an off-set value for the porosity dependence in Eq. (5), i.e., for each value of g, we let $\phi\rightarrow\phi-\phi(s=1,g)$. Such a proposal had already been suggested in the context of a percolation approach to porosity evaluation [26]. The second change refers to the formation factor S_0, which is defined as the ratio of the sum of obstacle perimeters to the area encircled by them. When the porosity change is due only to an increase in the number of identical obstacles, S_0 assumes a constant value but, in the present case, $S_0=\Theta(g)/s$, where $\Theta(g)=2\Sigma_{i=1}^{N_g} r_i/\Sigma_{i=1}^{N_g} r_i^2$, and the values of r_i are those of the original AP tangent circles. Thus, Eq. (5) must be rewritten as

$$\frac{k_g(s,g)}{k_0} = A\frac{s^2}{\Theta(g)^2}\frac{[\phi(s,g)-\phi(s=1,g)]^3}{[1-\phi(s,g)+\phi(s=1,g)]^2}. \tag{7}$$

The results shown in Fig. 4 clearly indicate that, with exception to large values of ϕ, the values of $k_g(s,g=\text{const.})$ align on straight lines for all values of s, when the right-hand side of Eq. (7) is evaluated for $g=$const. and decreasing values of s.

We investigated several properties of fluids in a channel with obstacles of different sizes, aiming to understand global effects on the flow induced by their presence. From a broader perspective, this work contributes to establishing limits to the validity of classical assumptions required for the derivation of semiempirical relationships of flows in porous media. It goes along with several studies that provide, with the help of CFD techniques, much finer analysis of the dependence of flow patterns in complex geometries by systematically solv-

ing the equations of fluid motion in their complete form with well defined boundary conditions. Other contributions have concentrated on the use of a large number of obstacles of the same size, randomly dispersed inside the channel, to model the porous media. In the current work, inhomogeneity is caused by obstacles of different sizes, ordered according to the AP. By uniformly reducing the different radii we are able to alter the value of porosity and permeability. We considered five different packing configurations, obtained by successively increasing the generation at which the Apollonian construction is stopped.

Our results indicate that the limit of validity of Darcy's law is very small ($\mathrm{Re}_{\max} \sim 6$ for small circles), but it increases both when the channels between obstacles have their width decreased, and the number of obstacles increases. Outside the range of validity of Darcy's law, our results for linear and quadratic corrections in the value of k allow for a good fitting quality. Our results for the dependence of the permeability on porosity show that the KC semiempirical relations is satisfied with a high decree of accuracy, provided we include the effect of a porosity offset due to fact that flow stops at a nonzero value of porosity.

Although we consider two-dimensional flows, our results are interesting enough to explore other packing geometries, in such a way to investigate the dependence of relative circle radii that are introduced in higher order generations. Studies in this direction are in progress.

The authors acknowledge the financial support of Brazilian agencies CNPq, CAPES, FINEP, FAPESB, and FUNCAP. J.S.A.Jr. and R.F.S.A. acknowledge the National Institute of Science and Technology for Complex Systems. Partial support from Petrobras is also acknowledged.

[1] A. E. Scheidegger, *The Physics of Flow through Porous Media*, 3rd ed. (University of Toronto Press, Toronto, 1974).
[2] J. Bear, *Dynamics of Fluids in Porous Media* (Dover, New York, 1988).
[3] F. A. L. Dullien, *Porous Media: Fluid Transport and Pore Structure* (Academic, New York, 1979).
[4] K. Aziz, *Petroleum Reservoir Simulation* (Applied Science Publishers LTD, London, 1979).
[5] D. Tiab and E. C. Donaldson, *Petrophysics: Theory and Practice of Measuring Reservoir Rock and Fluid Transport Properties*, 2nd ed. (Gulf Professional Publishing, Burlington, USA, 2004).
[6] R. B. Bird, W. E. Stewart, and E. N. Lightfoot, *Transport Phenomena*, 2nd ed. (Wiley, New York, 2001).
[7] H. K. Versteeg and W. Malalasekera, *An Introduction to Computacional Fluid Dynamics: The Finite Volume Method* (Longman Scientific & Technical, England, 1995).
[8] J. Tu, G. H. Yeoh, and C. Liu, *Computacional Fluid Dynamics: A Practical Approach* (Elsevier Science & Technology, New York, 2008).
[9] J. S. Andrade, D. A. Street, T. Shinohara, Y. Shibusa, and Y. Arai, Phys. Rev. E **51**, 5725 (1995).
[10] J. S. Andrade, M. P. Almeida, J. Mendes Filho, S. Havlin, B. Suki, and H. E. Stanley, Phys. Rev. Lett. **79**, 3901 (1997).
[11] H. E. Stanley, J. S. Andrade, S. Havlin, H. A. Makse, and B. Suki, Physica A **266**, 5 (1999).
[12] J. S. Andrade, Jr., U. M. S. Costa, M. P. Almeida, H. A. Makse, and H. E. Stanley, Phys. Rev. Lett. **82**, 5249 (1999).
[13] A. D. Araújo, W. B. Bastos, J. S. Andrade, Jr., H. J. Herrmann, Phys. Rev. E **74**, 010401(R) (2006).
[14] H. J. Herrmann, G. Mantica, and D. Bessis, Phys. Rev. Lett. **65**, 3223 (1990).
[15] J. Kozeny, Wasserkraft und Wasserwirtschaft **22**, 67 (1927).
[16] P. C. Carman, Trans. Inst. Chem. Eng. **15**, 150 (1937).
[17] P. C. Carman, J. Soc. Chem. Ind. **57**, 225 (1938).
[18] P. C. Carman, Discuss. Faraday Soc. **3**, 72 (1948).
[19] P. M. Adler, Int. J. Multiphase Flow **11**, 91 (1985).
[20] P. M. Adler, *Porous Media: Geometry and Transports* (Butterworth-Heinemann, Boston, 1992).
[21] J. C. Lagarias, C. L. Mallows, and A. Wilks, Am. Math. Monthly **109**, 338 (2002).
[22] R. L. Graham, J. C. Lagarias, C. L. Mallows, A. Wilks, C. H. Yan, J. Number Theory **100**, 1 (2003).
[23] FLUENT user manual (FLUENT Inc., Lebanon, New Hampshire, USA). FLUENT is a CFD package.
[24] GAMBIT user manual (FLUENT Inc., Lebanon, New Hampshire, USA). GAMBIT is a package to build mesh models for CFD and other applications.
[25] J. Andrade, Jr., A. Araújo, F. Oliveira, and A. Hansen, e-print arXiv:cond-mat/0608654.
[26] G. Mavko and A. Nur, Geophysics **62**, 1480 (1997).